RSC Advances

PAPER

View Article Online
View Journal | View Issue

Cite this: *RSC Adv.*, 2024, **14**, 3163

Graphitized mango seed as an effective 3D anode in batch and continuous mode microbial fuel cells for sustainable wastewater treatment and power generation

Nasser A. M. Barakat, *[a] Shimaa Gamal,[a] Zafar Khan Ghouri,[b] Olfat A. Fadali,[a] Omnia H. Abdelraheem,[c] Mohamed Hashem*[d] and Hager M. Moustafa[a]

Herein, we explored the utilization of graphitized mango seeds as 3D-packed anodes in microbial fuel cells (MFCs) powered by sewage wastewater. Mango seeds were graphitized at different temperatures (800 °C, 900 °C, 1000 °C, and 1100 °C) and their effectiveness as anodes was evaluated. Surface morphology analysis indicated that the proposed anode was characterized by layered branches and micro-sized deep holes, facilitating enhanced biofilm formation and microorganism attachment. Maximum power densities achieved in the MFCs utilizing the mango seed-packed anodes graphitized at 1100 °C and 1000 °C were 2170.8 ± 90 and 1350.6 ± 125 mW m^{-2}, respectively. Furthermore, the weight of the graphitized seed anode demonstrated a positive correlation with the generated power density and cell potential. Specifically, MFCs fabricated with 9 g and 6 g anodes achieved maximum power densities of 2170.8 ± 90 and 1800.5 ± 40 mW m^{-2}, respectively. A continuous mode air cathode MFC employing the proposed graphitized mango anode prepared at 1100 °C and operated at a flow rate of 2 L h^{-1} generated a stable current density of approximately 12 A m^{-2} after 15 hours of operation, maintaining its stability for 75 hours. Furthermore, a chemical oxygen demand (COD) removal efficiency of 85% was achieved in an assembled continuous mode MFC. Considering that the proposed MFC was driven by sewage wastewater without the addition of external microorganisms, atmospheric oxygen was used as the electron acceptor through an air cathode mode, agricultural biomass waste was employed for the preparation of the anode, and a higher power density was achieved (2170.8 mW m^{-2}) compared to reported values; it is evident that the proposed graphitized mango seed anode exhibits high efficiency for application in MFCs.

Received 27th July 2023
Accepted 8th December 2023

DOI: 10.1039/d3ra05084j

rsc.li/rsc-advances

1. Introduction

Microbial fuel cells (MFCs) have emerged as a promising technology for the sustainable generation of electricity *via* the utilization of microorganisms to catalyze the oxidation of organic matter. Furthermore, MFCs have potential applications in various fields, including wastewater treatment, environmental monitoring, and renewable energy production.[1–3] A critical aspect in the development of efficient MFC systems is the design and optimization of their anode electrode, which serves as the site for microbial attachment and electron transfer. Thus, it is necessary to explore highly efficient and biocompatible anode materials.

Currently, many available anode materials exhibit low electron transfer efficiency and poor biocompatibility, limiting the large-scale use of MFCs.[4,5] In this case, potential anode materials should have excellent biocompatibility, good conductivity, a large electrochemical active area, and low cost. Recently, anodes with diverse structures based on various materials have been studied for MFCs.[6,7] Standalone anodes, which can be derived from carbon materials, including graphite rod, felt, cloth, paper, and nanomaterials, are a popular choice in MFCs. However, despite their high mechanical stability and conductivity, these materials possess a small electrochemical active area, preventing bacterial growth due to fouling by bacterial secretions.[8,9] Recent research suggests that the use of carbon produced from natural biomass offers a potentially eco-friendly method for producing sustainable bioenergy from organic waste.

[a]*Chemical Engineering Department, Faculty of Engineering, Minia University, El-Minia 61516, Egypt. E-mail: nasbarakat@mu.edu.eg; Fax: +20862364420; Tel: +20862348005*

[b]*School of Computing, Engineering and Digital Technologies, Teesside University, UK*

[c]*Sciences Engineering Department, Faculty of Engineering, Beni-Suef University, Beni-Suef 62511, Egypt*

[d]*Dental Health Department, College of Applied Medical Sciences, King Saud University, Riyadh, 11433, Saudi Arabia. E-mail: mihashem@ksu.edu.sa*

Moreover, traditional anode materials, such as graphite and carbon cloth, have limitations in terms of cost, availability, and environmental impact.[10] Therefore, there is growing interest in exploring alternative, sustainable, and low-cost materials for the fabrication of MFC anodes. In this case, due to the abundance and potential of agricultural waste biomass for valorization, it has been considered a promising candidate for the preparation of anode materials.[11] Utilizing agricultural waste not only offers a solution for waste management but also provides a renewable and cost-effective source for the production of anode materials. Typically, the carbonization of plant precursors results in the production of porous carbon. Additionally, during the preparation process, plant heteroatoms (sulphur, nitrogen, silicon, phosphorous, *etc.*) act as natural advantageous dopants, resulting in the formation of self-doped materials that can improve the bioactivity of the prepared anode. Additionally, during the carbonization process, water evaporates and the byproduct gases from the graphitization of macro organic molecules create a porous structure in the carbon material, significantly increasing its surface area and bacterial attachment.[12,13] Consequently, a variety of biomasses, including loofah sponge,[14] corncob,[15] silkworm,[16] pinecone,[17] bread[32] and others,[18] have been used to create 3D anodes. However, in the case of the majority of reported anodes, an additional surface modification agent (such as polyaniline) was typically used. Furthermore, a simulated anolyte solution and a highly active electron acceptor, such as potassium ferricyanide ($K_3[Fe(CN)_6]$), were used in the cathode chamber to improve the generated power.

MFC anodes can be classified as planar, packed, or brush structures depending on how they are configured.[19] The types of planar structures include carbon paper and mesh, graphite plates or sheets, and carbon cloth or felt, among which some materials, such as carbon felt or mesh, have a greater specific surface area.[20–24] Alternatively, packed structures are becoming more popular in MFCs[25–27] because they offer a high surface area that is accessible to bacteria, are scalable, and are inexpensive. To achieve a high concentration of microorganisms per unit of volume, the anode chamber of the MFC can be filled with granular or irregularly shaped packing scaffolds, similar to the biological filter for wastewater treatment.[28,29] For example, packed anodes consisting of granular activated carbon, granular graphite, and carbonized natural materials can produce adequate electricity-generating performances with low overall cost in MFCs.[27,30,31] In this case, the granular packing material must be conductive in the MFC, for example, granular graphite and active carbon.[28,32,33] The granules must be closely packed adjacent to each another to make the entire bed conductive, while dead zones for current collection may exist after long-term operation. Due to their density and low potential for clogging, packed granules are frequently utilized in MFC investigations despite the possibility of biofouling.[19,34,35] Also, the materials of packed anodes frequently need to be tightly packed for conductive contact, which results in less space between the packing materials. Thus, to prepare packed anodes with long-term stability and good electricity-generating capability, suitable packing materials are desirable.[36,37]

In this context, mango seeds, as common agricultural waste products, have recently gained attention for their potential as anode materials in MFCs. Mango seeds possess a complex hierarchical structure that can be graphitized through heat treatment, resulting in enhanced electrical conductivity and surface characteristics favorable for biofilm formation.[38–40] Furthermore, graphitization of the mango seed anode creates a pseudo-graphitic carbon structure, which can facilitate efficient electron transfer during the microbial oxidation process.[41] Moreover, the graphitization of mango seeds can be controlled to maintain their mechanical properties as a 3D-packed anode in MFCs.

To optimize the performance of graphitized mango seed anodes, the calcination temperature during the graphitization process is a crucial parameter. Different calcination temperatures can lead to variations in the structural and electrochemical properties of the resulting anodes. Thus, understanding the impact of calcination temperature on the performance of graphitized mango seed anodes is essential for their successful application in MFCs.

In this study, we investigated the influence of different calcination temperatures (800 °C, 900 °C, 1000 °C, and 1100 °C) on the characteristics and performance of graphitized mango seed anodes in MFCs driven by sewage wastewater. Subsequently, we evaluated the surface morphology, crystalline structure, elemental composition, electrical resistance, power density, stability, and COD removal efficiency of the MFCs. Additionally, we explore the relationship between anode weight and power density. The findings from this study can contribute to the understanding of the potential of graphitized mango seed anodes for efficient electricity generation in MFCs.

2. Materials and methods

2.1 Materials

Biomass carbon derived from mango seed materials were acquired and used as packed anodes, while Pt-loaded carbon cloth (0.5 mg cm^{-2}, Electro Chem Inc., USA) served as the cathode in all tests. In the El-Minya Governorate, Egypt, there is a long (135 km) water drain (MASRAF Al-MOHEET), receiving around 9000 m^3 per day industrial, municipal and agriculture wastewaters. These polluted wastewaters are poured into the Nile River without treatment, which creates dangerous environmental problems. The proposed microbial fuel cell in this study was established to work using this wastewater. Samples were collected from this water drain and characterized in the Sanitation and Drinking Water Company Labs, El-Minya, Egypt. It was considered that this wastewater was relatively aerobic treated given that the samples were collected from a flowing-water drain. The results are summarized in Table 1.

The total bacteria count was estimated using the following procedure: the as-collected sewage water was filtered to remove solid particles. Subsequently, 1 mL of the filtered water was added to 9 mL of sterilized water, shaken for 5 min, the solution was diluted (10^{-1} to 10^{-6}), and then the resulting solutions were plated directly on the surface of nutrient agar.[42] The agar was incubated at 25 °C or 30 °C for 10 days, and then the colony

Table 1 Chemical characterization of the utilized wastewater[a]

pH	COD (mg L^{-1})	BOD (mg L^{-1})	TSS (mg L^{-1})	TDS (mg L^{-1})	Total P (mg L^{-1})	VSS (mg L^{-1})	Total N (mg L^{-1})	Alk (mg L^{-1})
7.45 ± 0.03	305 ± 15	269 ± 5	65 ± 5	554 ± 17	3.594 ± 0.01	155 ± 3	4.3 ± 0.15	235 ± 7

[a] COD: chemical oxygen demand. BOD: biological oxygen demand. TSS: total suspended solids TDS: total dissolved solid. Total P: total phosphorus content. VSS: volatile suspended solids. Total N: total nitrogen content. Alk: total alkalinity.

forming units (CFU) were counted. Data analysis was done using the SAS statistical programme (SAS Institute, Cary, NC, USA). Tukey's estimates of honest significant differences (HSD) were computed from the ANOVA analysis when a significant F value was found. A statistical significance of 0.05 and 0.01 was established. The formula used to compute counts was $y = \log(x + 1)$, where x is the initial CFU mL^{-1} sample of sewage water. The results indicated that the number of bacteria in the used sewage was 10^6–10^7 CFU mL^{-1}.

2.2 Preparation of biomass carbon for anode

Mango seeds were gathered from rural areas, lightly polished, and then meticulously cleaned with clean water to get rid of any contaminants. The carbonization procedure was carried out in an inert atmosphere in a tube furnace at a heating rate of 2 °C min^{-1} with a holding time of 3 h at several calcination temperatures (800 °C, 900 °C, 1000 °C, and 1100 °C) after drying at 80 °C overnight. The procedure for the preparation of the anode packed structure from mango fruit is summarized in Fig. 1. As can be seen in the photograph, the graphitized seeds were tightly inserted in a high corrosion resistance stainless steel envelope, which was served as the current collector.

2.3 MFC operations and configurations

In the batch mode, a membrane-less single chamber MFC with a carbon cloth Pt-loaded (0.5 mg cm^{-2}) cathode was used. In the 80 mL volume anode chamber, the graphitized mango seed-contained stainless steel bucket was deluged in a sewage wastewater previously purified by nitrogen bubbling for 10 min. At the cathode side, a stainless steel sheet with high corrosion resistance was utilized as the current collector. All experiments were performed at room temperature. Under anaerobic conditions, in the batch-mode MFC, the cell was operated to immobilize the microorganisms on the anode for a specific time until the open circuit voltage (OCV) was stabilized and equilibrium of the two half reactions was established. The cell potential was captured using a GL220 midi-logger. The anode and cathode potentials were measured using a reference electrode (Ag/AgCl). The generated power density was measured *via* linear sweep voltammetry (LSV) at a scan rate of 1 mV s^{-1}. In the electrochemical measurements, the working electrode was connected to the cathode, while the counter electrode and reference electrodes were linked with the MFC anode. A potentiostat/galvanostat (HA-1516, Japan) device was used to monitor the current (at 0 V) to investigate the stability of the continuous mode cell, which was operating at a flow rate of 2 L h^{-1} using

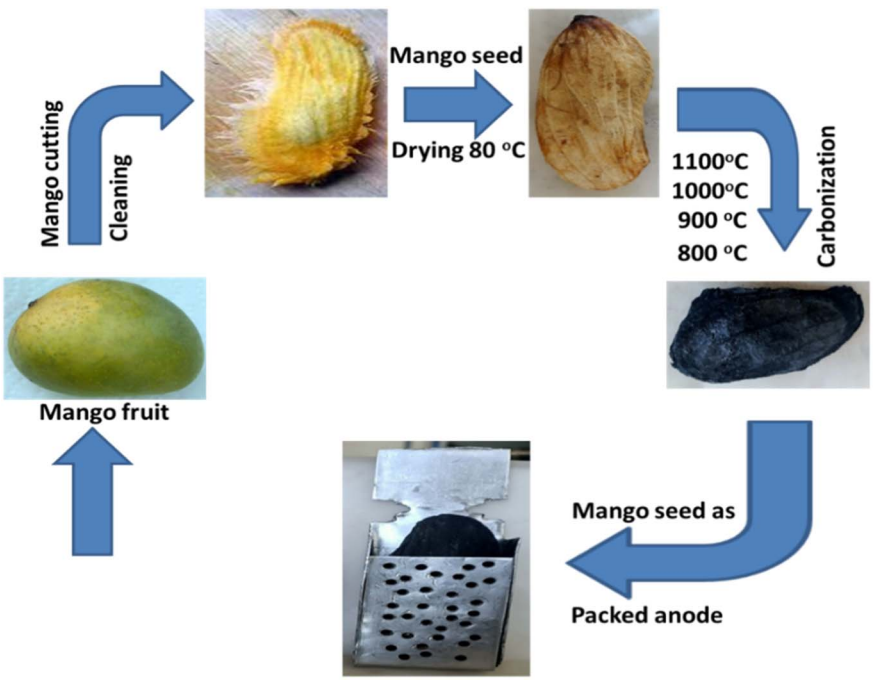

Fig. 1 Schematic diagram of the procedure for the preparation of the anode packed structure from mango fruit.

a peristaltic pump. The current and power densities were adjusted to the cathode area. Sodium acetate (5 g L^{-1}) was added to the anolyte solution to elevate the COD, improve the performance and reduce the power overshoot.[38] To measure the variation in the COD, samples were taken from the MFC every day, while the current density was measured after OCV stabilization in a continuous-mode MFC.

2.4 Characterization

The surface morphology of the prepared anode material was analyzed *via* scanning electron microscopy (SEM JSM-IT200, JEOL, Japan). X-ray diffraction was performed on a Rigaku instrument (XRD, Japan) to characterize the chemical composition of the proposed anode. Utilizing a VersaStat4 potentiostat (AMETEK Scientific Instruments, USA) and a two-electrode setup with the anode serving as both the counter and reference electrode and the cathode serving as the working electrode, linear sweep voltammetry (LSV) was performed to obtain the polarization curves at a scan rate of 1 mV s^{-1}.

3. Results and discussion

3.1 Characterization of the anode

Biomass carbonization can be understood as gas evolution reactions. The moisture content from lignin is removed during the carbonization process, and the inorganic components produce volatile chemicals, which undergo condensation to generate a porous framework.[43,44] This hypothesis was supported scientifically by the scanning electron microscopy analysis, as shown in Fig. 2. The SEM image of the graphitized mango seeds revealed important insight into the morphological characteristics of the resulting surface after carbonization (Fig. 2A). One notable observation is that the initial morphology of the mango seeds was not destroyed during the carbonization process. This indicates that the graphitization treatment preserved the overall structure of the mango seeds, allowing for their potential utilization as anodes in microbial fuel cells (MFCs).

The presence of several layered branches on the surface of the graphitized mango seeds is an encouraging feature. These layered branches created a highly porous and complex surface structure, which is advantageous for biofilm formation in MFCs. The increased surface area provided by the layered branches offers ample attachment sites for microorganisms, facilitating their colonization and growth on the anode surface. The formation of a biofilm is crucial for efficient electron transfer and the overall performance of MFCs, given that it establishes a conductive network of microorganisms capable of facilitating the transfer of electrons generated during the oxidation of organic matter.

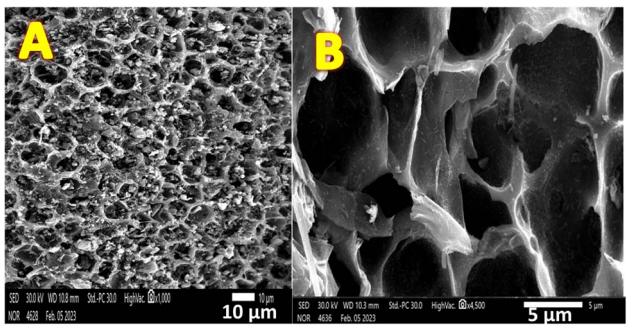

Fig. 2 Low (A) and high (B) magnification SEM images of the surface of the carbonized mango seed at 1100 °C.

Additionally, the high magnification image (Fig. 2B) further highlights another important aspect of the graphitized mango seed surface, *i.e.*, the presence of micro-size deep holes. These holes significantly contribute to the overall surface area available for the attachment of microorganisms. The increased surface area created by the micro-size deep holes enhances the colonization of microorganisms, given that it provides additional sites for their adhesion and growth. Furthermore, the three-dimensional nature of the surface, characterized by layered branches and deep holes, promotes the establishment of a biofilm with a complex and interconnected structure, which can further enhance the efficiency of electron transfer processes.

The observed surface characteristics of the graphitized mango seeds are consistent with the desirable attributes of an effective anode material in MFCs. The combination of layered branches and micro-size deep holes provides a highly favorable surface for biofilm development, which is essential for the performance of MFCs. The enhanced biofilm formation on the anode surface facilitates the establishment of a robust microbial community capable of efficiently oxidizing organic matter and transferring electrons to the anode. The preservation of the morphology of the mango seeds during graphitization highlights their potential as a sustainable and effective material for 3D anode applications in MFCs driven by sewage wastewater.

The XRD pattern presented in Fig. 3 provides valuable information regarding the crystalline structure of the proposed mango seed anode prepared at 1100 °C. The identification of the characteristic peaks centered at the 2θ values of 24° and 43°, corresponding to the (002) and (100) lattice planes, respectively, confirms the formation of pseudo-graphitic carbon. This finding suggests that the heat treatment process during the graphitization of the mango seed anode led to the development of a graphitic-like structure.[45]

The presence of these characteristic peaks in the XRD pattern indicates the alignment of the carbon atoms in a layered structure, similar to the arrangement found in graphitic materials. This graphitic-like structure enhances the electrical conductivity of the anode, given that it facilitates the movement of electrons through the material.[46] The formation of pseudo-graphitic carbon in the mango seed anode is advantageous for its utilization in microbial fuel cells (MFCs) because it promotes efficient electron transfer from the microorganisms to the anode surface.

The findings of this study demonstrate that a high pyrolysis temperature, such as 1100 °C, is beneficial for the pseudo-graphitization of the mango seed anode. The graphitization process enhanced the electrical conductivity of the anode, leading to improved electron transfer capabilities. The

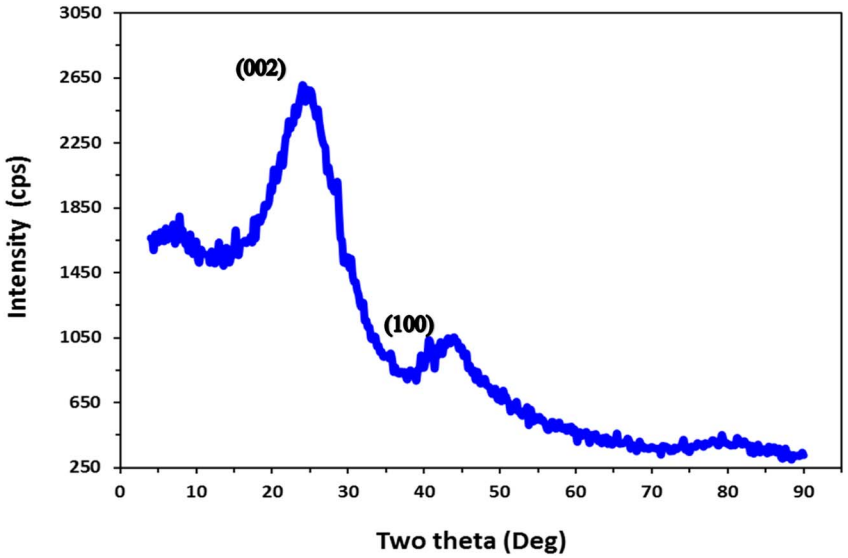

Fig. 3 X-ray pattern of mango seed anode carbonized at 1100 °C.

increased conductivity allows for the more efficient utilization of the electrons generated during the microbial oxidation process in MFCs. Therefore, the choice of an appropriate pyrolysis temperature is crucial in optimizing the electrical properties of the anode material. These results highlight the significance of the graphitization process and emphasize the importance of high pyrolysis temperature in enhancing the conductivity and overall effectiveness of the proposed mango seed anode in MFC applications.[44,47–49]

The EDS analysis presented in Fig. 4 provides insights into the elemental composition of the mango seed anode after carbonization at 1100 °C. The results, as shown in Table 2, indicate the percentage of different elements present in the mango seed material. Notably, carbon exhibited the highest percentage among the elements, which was expected given that carbon is the primary constituent of the anode material.

The high percentage of carbon in the mango seed anode is advantageous for its performance in microbial fuel cells (MFCs). Carbon is known for its excellent electrical conductivity, making it an ideal material for facilitating electron transfer in electrochemical systems. In the context of MFCs, efficient electron transfer from the microorganisms to the anode surface is critical for achieving high power densities. Therefore, the presence of a high carbon content in the mango seed anode contributed to its effectiveness in facilitating electron transfer during the microbial oxidation process.

In contrast, the percentage of oxygen (O), silicon (Si), phosphorus (P), potassium (K), and calcium (Ca) showed a significant decrease after the carbonization process, which can be attributed to their conversion into gaseous byproducts or volatilization during the high-temperature treatment. The carbonization process involves the removal of non-carbonaceous elements from the mango seed material, resulting in a higher

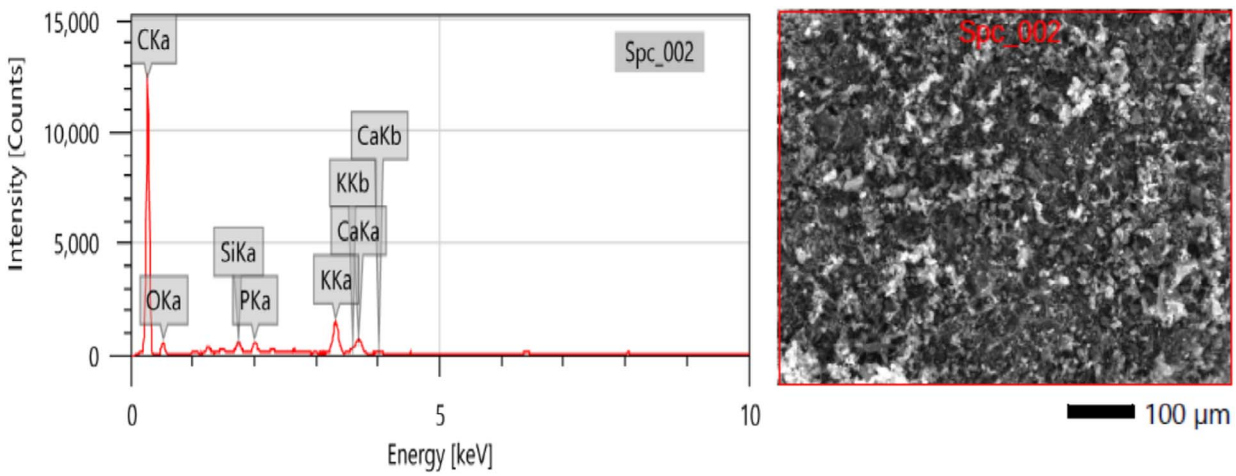

Fig. 4 EDS mapping of the mango seed calcined at 1100 °C.

Table 2 EDS analysis of the mango seed calcined at 1100 °C

Element	C	O	Si	P	K	Ca
Mass (%)	80.69 ± 0.16	14.75 ± 0.27	0.52 ± 0.01	0.66 ± 0.02	2.31 ± 0.03	1.06 ± 0.02

carbon content and a more concentrated carbon structure. This observation supports the notion that the graphitization process effectively transforms the mango seed material into a carbon-rich structure, enhancing its electrical conductivity and suitability as an anode material for MFCs.

The electrical conductivity measurements of the produced anode using a two-electrode setup, as illustrated in Fig. 5, provided valuable insights into the conductivity characteristics of the graphitized mango seed anode. The measurements were conducted through current–voltage (*I–V*) plots at various points on the anode surface. Remarkably, perfect linear relationships between the applied voltage and current were observed, indicating that the electrical conductivity of the produced anode is comparable to that of metals.

The linear relationship between voltage and current in the *I–V* plots suggests that the graphitized mango seed anode exhibits metallic-like conductivity. This is a highly desirable property for anodes in microbial fuel cells (MFCs), given that it allows efficient electron transfer from the microorganisms to the anode surface. The metallic-like conductivity facilitates the rapid movement of electrons through the anode material, enabling the efficient transfer of the electrical charge generated during the microbial oxidation process. The measured electrical resistances further support the fast electron transfer process observed in the *I–V* plots. The average electrical resistance across the investigated samples was determined to be 11.59 ohm cm^{-1}, which is equivalent to 8.6 Siemen m^{-1}. This relatively low resistance indicates that the graphitized mango seed anode possesses excellent electrical conductivity, contributing to its effectiveness in MFC applications.

The results suggest that the pyrolysis temperature plays a crucial role in optimizing the electrical conductivity of the anode material. The high pyrolysis temperature of 1100 °C likely enhanced the graphitization process, resulting in the formation of a more conductive carbon structure. Consequently, the anode prepared at this temperature exhibited enhanced electrical resistance and conductivity, further supporting its suitability for MFCs.

In contrast, the anode obtained at 800 °C exhibited relatively lower electrical conductivity, with an electrical resistance of 6.9 Siemen m^{-1}. This result suggests that the pyrolysis temperature influences the quality of the graphitized structure, and subsequently the electrical properties of the anode material. The lower conductivity observed at 800 °C indicates a less efficient electron transfer process, which may result in a decreased power output in MFCs.

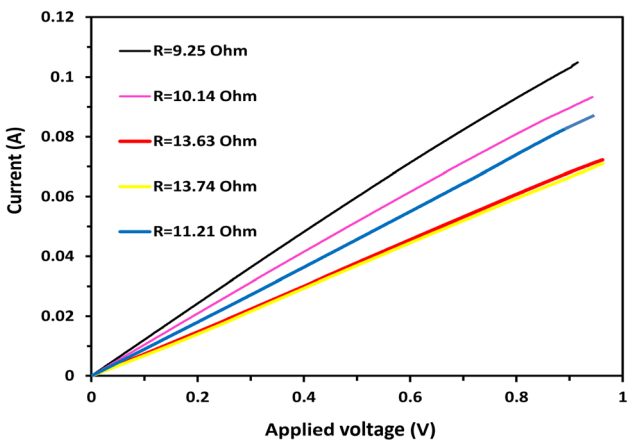

Fig. 5 *I–V* relationship for the mango seed carbonized at 1100 °C. The measurement was conducted using a 1 cm two-electrode setup at 5 different locations on the same anode.

3.2 Anode performance in batch mode MFCs

The physicochemical characteristics of the proposal anodes were influenced by their graphitization temperature, which is an important aspect to be studied. Thus, to investigate the influence of this important factor, the mango seed was prepared as a packed anode structure at four different temperatures of 800 °C, 900 °C, 1000 °C and 1100 °C. The proposed anodes were used to pack four MFCs. Fig. 6 illustrates the performance of the assembled cells. It can be seen from the polarization curves (Fig. 6A) that the anodes prepared at 1100 °C and 1000 °C showed a good performance, whereas that prepared at 900 °C and 800 °C exhibited a low performance. Fig. 6B presents a numerical representation of the maximum power density obtained from the assembled MFCs using the mango seed-packed anodes graphitized at different temperatures. As shown, the generated power densities from the anodes calcined 1100 °C and 1000 °C were 2170.8 ± 90 and 1350.6 ± 125 mW m^{-2}, respectively. However, when the calcination temperature was lowered to 900 °C and 800 °C, the maximum power density was reduced to 895.4 mW m^{-2} and 542.6 mW m^{-2}, respectively. This result can be explained by the variations in the electrical conductivities of the prepared anodes.[38]

The observation that the 1000 °C anode required 7 days to reach its maximum power density (Fig. 6C), while the MFCs based on the anodes calcined at 1100 °C, 900 °C, and 800 °C achieved their highest power densities after 6 days of operation, provides interesting insights into the performance and stability of the different anode materials in microbial fuel cells (MFCs).

The time required to reach the maximum power density can be influenced by various factors, including the initial biofilm formation, establishment of an efficient electron transfer network, and adaptation of the microorganisms to the anode surface. The delayed attainment of the maximum power density for the anode calcined at 1000 °C suggests that it might have required additional time for the biofilm to develop, electron transfer pathways to be established, and the microbial

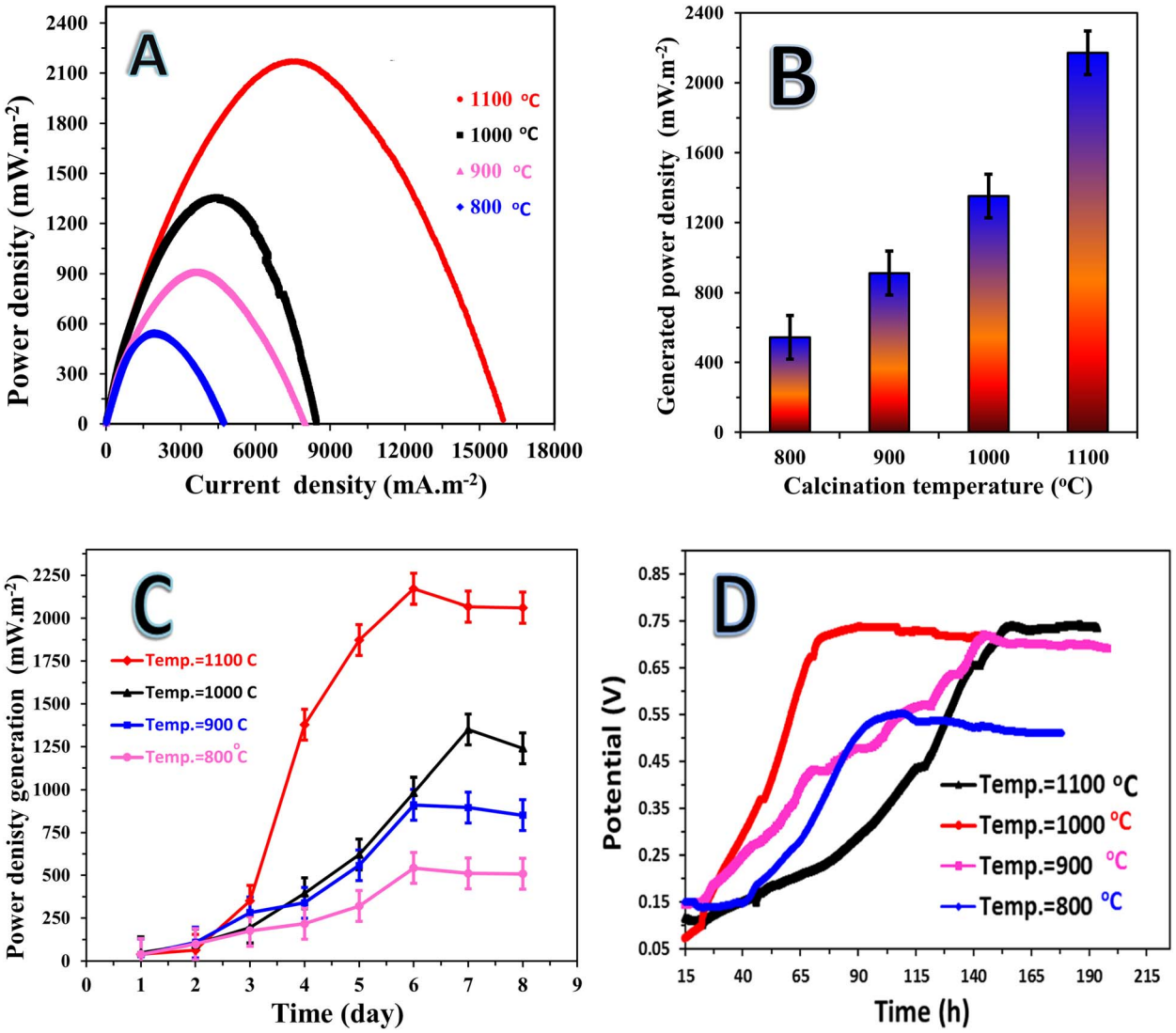

Fig. 6 Influence of mango seed calcination temperature on the performance of NaAc (5 g L^{-1})/sewage wastewater-based microbial fuel cells. (A) Polarization curves of the assembled microbial fuel cells, (B) maximum generated power densities at different calcination temperatures, (C) influence of running time on the generated power, and (D) change in the open cell potential with respect to time.

community to adapt to the anode surface. This slower initial performance may have been due to the specific surface characteristics or structural properties of the anode calcined at 1000 °C, which could have affected the attachment and growth of microorganisms. In contrast, the MFCs based on the anodes calcined at 1100 °C, 900 °C, and 800 °C achieved their highest power densities after 6 days of operation. This relatively shorter timeframe indicates that these anode materials facilitated more rapid biofilm formation, electron transfer network establishment, and microbial adaptation. The surface characteristics, such as the layered branches and micro-size deep holes observed in the SEM images, likely played a crucial role in providing favorable attachment sites for microorganisms and promoting biofilm development. The enhanced biofilm formation on these anodes created an effective conductive network, allowing efficient electron transfer and power generation. These findings emphasize the importance of optimizing the anode material and its surface characteristics to promote efficient biofilm formation and electron transfer, ultimately leading to improved power generation in MFCs.

The study on the variation of the open circuit potential (OCP) with time for assembled microbial fuel cells (MFCs) provided important insights into the electrochemical behavior and stability of the different MFC systems, as shown in Fig. 6D. The results indicate that the MFC with the 1000 °C-anode achieved the fastest OCP stabilization, with the OCP rapidly increasing over time to reach a value of 0.75 V within 63 h of operation. This suggests that the 1000 °C-anode MFC had favorable electrochemical properties, allowing for efficient electron transfer and establishment of an electrochemical potential. The rapid increase in OCP indicates good biofilm formation and electron transfer kinetics, leading to a stable and high potential difference between the anode and cathode.

In contrast, the 900 °C- and 1100 °C-anode MFCs reached their maximum OCP values at approximately the same time of around 140 h. However, there were differences in the rate of OCP increase between these two systems. In the case of the 900 °C-anode MFC, its OCP increased steadily at a relatively constant rate, suggesting more consistent and controlled electrochemical behavior. Alternatively, the 1100 °C-anode MFC exhibited a slower initial increase in OCP, followed by a sharp rise. This behavior indicates a gradual buildup of biofilm and electron transfer capabilities on the anode surface, followed by an acceleration in the electrochemical processes. The maximum OCP values achieved for the 900 °C- and 1100 °C-anode MFCs were 0.73 V and 0.75 V, respectively. These values indicate relatively high OCP levels, suggesting efficient electron transfer and favorable electrochemical performances. The slight difference in the maximum OCP values between the two systems can be attributed to variations in the anode characteristics, such as surface morphology, carbon structure, and elemental composition, resulting from the different carbonization temperatures.

The MFC assembled with the 800 °C-anode exhibited the lowest maximum OCP of 0.54 V, which was achieved after 113 h of operation. This lower OCP value is associated with the less favorable electrochemical properties of the 800 °C-anode, such as reduced conductivity and less efficient biofilm formation.[50] The lower OCP suggests lower electron transfer efficiency and a less favorable redox potential difference between the anode and cathode.

Overall, the variation in OCP with time for the different MFCs provides insights into their electrochemical performance and stability. The rapid OCP stabilization observed for the 1000 °C-anode MFC indicates its superior electrochemical properties, while the differences in the rate of OCP increase and maximum OCP values for the 900 °C -and 1100 °C-anode MFCs highlight the influence of the carbonization temperature on the anode performance. The lower maximum OCP value for the 800 °C-anode MFC suggests less efficient electron transfer and lower electrochemical potential.

The SEM images presented in Fig. 7 provide visual evidence of the changes occurring on the surface of the 1100 °C-anode before and after usage in the microbial fuel cell (MFC). The comparison between the fresh and used anode surfaces revealed important insights into the biofilm formation and microorganism colonization. As shown in Fig. 7A, the SEM image of the fresh 1100 °C-anode surface displayed numerous open and deep pores. These pores create a highly porous and complex surface structure, which is advantageous for biofilm formation in MFCs. The presence of these pores provides ample attachment sites for microorganisms, enabling their colonization and growth on the anode surface.

As shown in Fig. 7B, the SEM image of the used 1100 °C-anode surface demonstrated the changes that occurred after the anode was utilized in the MFC. The previously observed open and deep pores were filled with numerous microorganisms, indicating the successful colonization and attachment of the microorganisms to the anode surface. The microorganisms occupied the available spaces in the pores, creating a densely packed biofilm. This biofilm formation is crucial for the effective functioning of the MFC, given that it enables the microorganisms to engage in the oxidation of organic matter and facilitates the transfer of electrons to the anode.

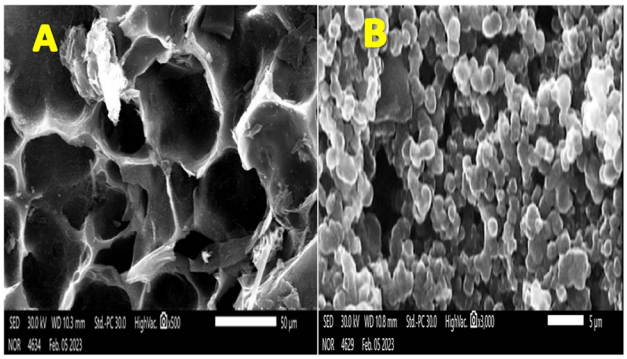

Fig. 7 SEM images of the 1100 °C-mango seed anode (A) before use in an MFC and (B) showing the attached microorganisms on the surface of the proposed anode after use in an MFC.

The presence of microorganisms in the pores of the used anode surface indicates the formation of a mature and well-established biofilm. The densely packed biofilm ensures a large population of microorganisms, which enhances the overall electrochemical performance of the MFC. The biofilm acts as a conductive pathway, allowing for efficient electron transfer from the microorganisms to the anode surface. The establishment of a conductive biofilm network is crucial for achieving high power densities in MFCs.

The SEM images in Fig. 7 highlight the successful colonization and growth of microorganisms on the surface of the 1100 °C-anode. The presence of open and deep pores in the fresh anode surface provides an ideal environment for biofilm formation, while the filling of these pores with microorganisms in the used anode indicates a successful colonization process. The formation of a well-developed biofilm promotes efficient electron transfer and supports the stable and continuous operation of the MFC.

The study on the effect of anode weight on the performance of the graphitized mango seed anode in microbial fuel cells (MFCs) provided valuable insights into the relationship among the anode weight, power density, open circuit potential (OCP), and stabilization time, as shown in Fig. 8. The results indicate that an increase in the weight of the anode had a positive impact on the maximum power density achieved in the MFCs. In the case of the anode graphitized at 1100 °C, the MFCs assembled with the mango seed packed anodes weighing 9 g and 6 g achieved the maximum power densities of 2170.8 ± 90 mW m^{-2} and 1800.5 ± 40 mW m^{-2}, respectively. This suggests that a higher anode weight provides more surface area for biofilm formation and facilitates a greater number of microbial attachment sites, resulting in enhanced power generation.

The stabilization time of the power density in the MFCs is also influenced by the anode weight. As shown in Fig. 8C, a higher anode weight led to a shorter stabilization time. The MFC with the 9 g anode reached its maximum power density within 5 days, while the MFC with the 6 g anode achieved its

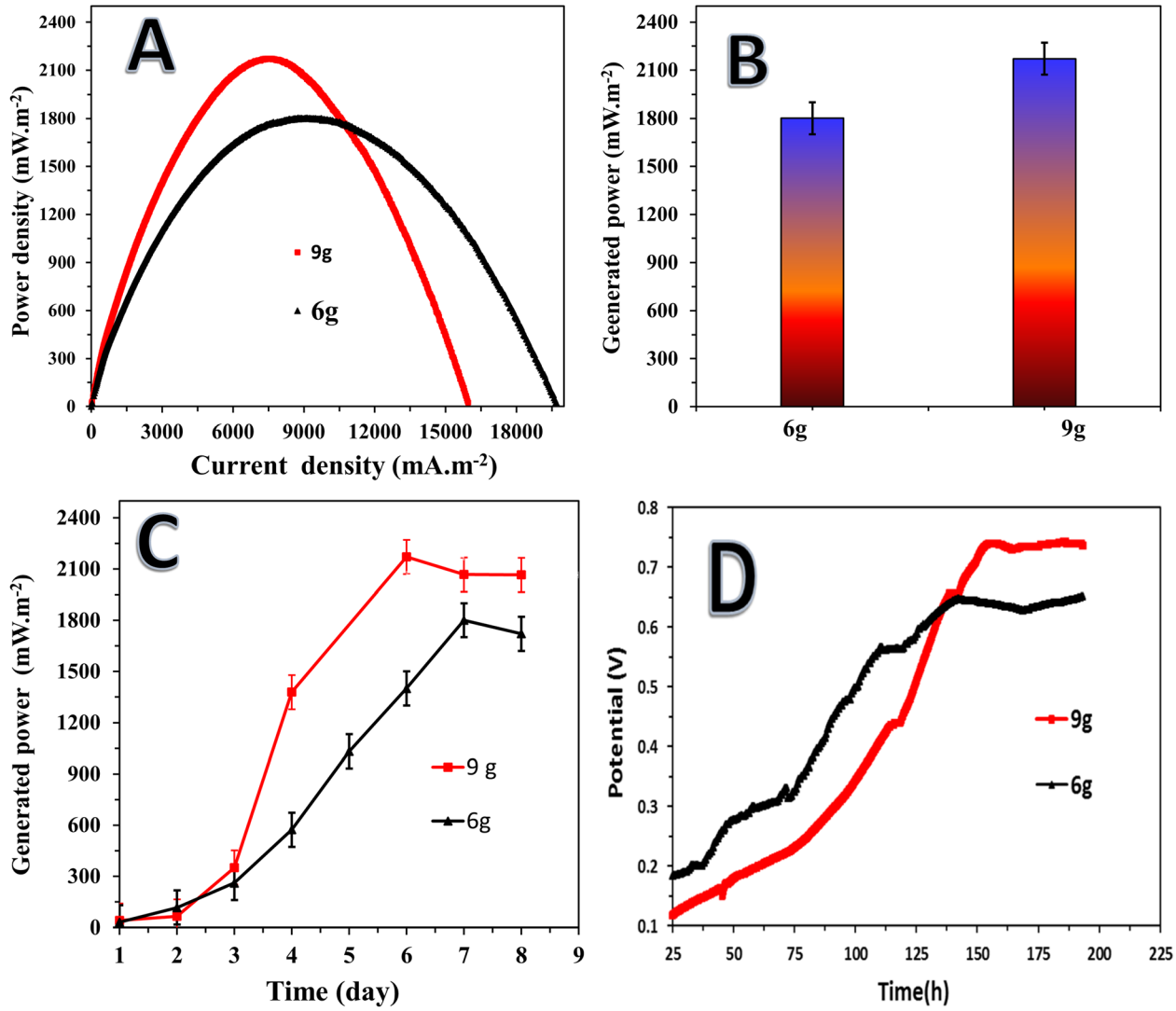

Fig. 8 Performance of 9 and 6 g 1100 °C-mango seed anodes. (A) Polarization curves of the assembled microbial fuel cells, (B) maximum generated power using the investigated anodes, (C) influence of running time on the generated power, and (D) change in the open cell potential with respect to time.

maximum power density within 7 days. This implies that a higher anode weight promotes a more rapid establishment of an efficient microbial community and electron transfer network, leading to faster power density stabilization.

The change in OCP over time, as depicted in Fig. 8D, further illustrates the effect of anode weight on the MFC performance. In both formulations, the OCP initially increased rapidly with time until reaching a certain point. Subsequently, the OCP stabilized at a relatively constant value. The maximum OCP achieved was also found to be dependent on the anode weight, with values of 0.66 V and 0.765 V observed for the 9 g and 6 g anodes, respectively. Additionally, the time required to reach the maximum OCP was longer for the 9 g anode (137 h) compared to the 6 g anode (153 h). The relationship between anode weight and MFC performance can be attributed to several factors. Increasing the anode weight provides a larger surface area for biofilm formation and microbial attachment, enhancing the electron transfer capabilities of the MFC. The greater availability of attachment sites promotes the establishment of a more diverse and active microbial community, resulting in improved power generation. Additionally, a higher anode weight may contribute to better nutrient and electron transfer in the MFC system.[51]

Overall, the study on the effect of anode weight on the performance of the graphitized mango seed anode in MFCs highlighted the positive correlation among the anode weight, power density, OCV, and stabilization time. An increase in the anode weight led to higher maximum power densities, shorter stabilization times, and higher maximum OCV values. These findings emphasize the importance of optimizing the anode weight to enhance the performance and stability of MFCs driven by sewage wastewater, ultimately contributing to more efficient electricity generation from agricultural biomass waste.

The results obtained from the cyclic voltammetry (CV) measurements, as presented in Fig. 9, provide significant insights into the electrochemical characteristics of the proposed graphitized mango seed anodes for their application in microbial fuel cells (MFCs). In the CV experiments, the absence of redox peaks in the voltammogram indicated that the anode surface was devoid of electrochemically active species. This observation effectively characterizes the anode as electrochemically inert. The electrochemical inertness of the anode has important implications for the mechanisms of electricity generation in the assembled MFCs. The absence of redox peaks implies that there were no distinct electrochemical reactions taking place on the anode surface under the experimental conditions. In traditional electrochemical systems, the presence of redox peaks in CV measurements indicate the presence of electrochemically active sites where specific reactions occur, typically involving the transfer of electrons between the electrode and solution-phase species.

In the context of MFCs, electrochemically active sites on the anode would potentially participate in the electron transfer reactions between the anode and the microorganisms present in the system. These reactions are pivotal for electricity generation in MFCs. Commonly, redox peaks in CV experiments for MFC anodes suggest the presence of electron transfer mediators or redox-active functional groups on the anode surface, facilitating direct or mediated electron transfer to and from the microorganisms.

However, the electrochemical inertness of the graphitized mango seed anode, as evidenced by the absence of redox peaks, strongly supports the conclusion that the electricity generated in the assembled MFC is predominantly attributed to biological oxidation processes. In this case, the microorganisms actively engage in the direct or mediated electron transfer to the anode surface as part of their metabolic activities. They utilize the anode as an electron acceptor, thereby contributing to the generation of electrical current. This outcome is consistent with the core principles of MFCs, where microorganisms, often termed exoelectrogens, participate in the microbial oxidation of organic pollutants in wastewater. During this process, they release electrons as metabolic byproducts. Subsequently, these electrons are harnessed by the anode to generate electricity. The electrochemical inertness of the anode surface, as revealed by the CV measurements, highlights that the graphitized mango seed anode primarily served as an electron acceptor for microbial metabolism, further corroborating the central role of microorganisms in electricity generation in MFCs.

In summary, the CV results provide compelling evidence that the electricity generation in the assembled MFCs is fundamentally driven by the biological oxidation of organic pollutants through the exoelectrogen microorganisms. This finding highlights the ecological and sustainable aspects of MFC technology, given that it harnesses the natural metabolic processes of microorganisms to achieve wastewater treatment and power generation simultaneously.

Additionally, the elemental analysis of the graphitized mango seeds showed that carbon and oxygen are the major elements, with other detected elements present in trace amounts. This suggests the minimal alteration in the elemental composition of the anode after utilization in the MFC. Considering these results, it is believed that the proposed graphitized mango seed anode exhibited excellent stability and biocompatibility, as evidenced by the lack of significant changes in its surface properties and elemental composition post MFC operation.

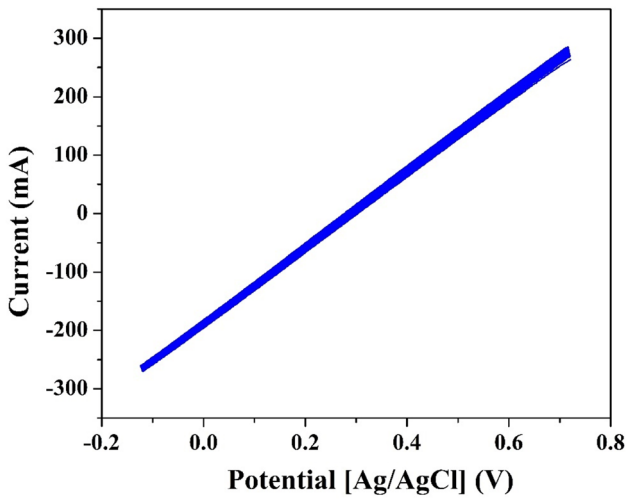

Fig. 9 Cyclic voltammetry measurement using the mango seeds graphitized at 1100 °C as the anode, graphite rod as the cathode and sewage water/sodium acetate as the electrolyte. The measurement was performed at 25 °C and scan rate of 5 mV s^{-1}.

3.3 Electrochemical impedance spectroscopy measurement

Electrochemical impedance spectroscopy (EIS) is a powerful tool used to investigate and understand the electrochemical processes occurring in microbial fuel cells (MFCs). It provides valuable information about the power delivery capabilities, performance, and internal resistance of MFC systems. EIS allows for the determination of the internal resistance of an MFC. This resistance includes the combined effect of ionic resistance, charge transfer resistance, and mass transfer resistance in the system. By analyzing the impedance spectra obtained from EIS measurements, it is possible to extract information about the different components contributing to the internal resistance. This characterization helps in understanding the limitations and factors that affect the power delivery capabilities of the MFC. In general, EIS measurements are essential for understanding the power delivery capabilities of microbial fuel cells. By characterizing the internal resistance, identifying electrochemical processes, evaluating the mass transport limitations, monitoring biofilm formation, and assessing electrode stability, EIS provides critical insights into the factors influencing the MFC performance. This knowledge can be utilized to optimize the design, operation, and electrode materials of MFCs, ultimately enhancing the power output and advancing the practical application of MFC technology.

To maintain homogeneity, the EIS measurements were carried out in the fully charged state after reaching the

stabilization state in the batch-mode MFC with 1100 °C- (Fig. 10A) and 900 °C- (Fig. 10B) mango seed anode. In general, the high-frequency semicircle and semicircle in the medium frequency region are ascribed to the surface interface layer resistance (SEI) and/or contact resistance, and the charge-transfer impedance at the electrode–electrolyte interface, respectively.[52,53] The linear part of the spectrum is assigned to the Warburg impedance, which is specified as the diffusion of certain ions into the bulk of the electrode materials.[54] The charge transfer resistance (R_{ct}) of the utilized mango seed electrodes was 20.3 and 22.5 ohm for the 1100 °C and 900 °C anodes, respectively, based on the modified Randles equivalent circuit illustrated in the inset of Fig. 10A, which is considered a low value signifying a quick charge transfer process. Furthermore, the SEI resistance (R_s) of the prepared electrodes (32 and 37.5 ohm for 1100 °C and 900 °C anodes, respectively) was also low, indicating that the two electrodes have good electronic and ionic conduction. It is well known that improved electrical and ionic conduction lead to a better electrochemical performance.[52]

3.4 Continuous-mode MFC

The continuous mode microbial fuel cell (MFC) experiment, utilizing the anode graphitized at 1100 °C, provided important insights into the stable current density generated by the MFC system under specific operating conditions. The setup of the MFC, as illustrated in Fig. 11A, included a storage tank, peristaltic pump, MFC, data logger, and potentiostat adjusted at 0 V applied voltage and helped to monitor the generated current. The wastewater was supplemented with sodium acetate at a concentration of 5 g L^{-1} and a constant flow rate of 2 L h^{-1} was maintained throughout the experiment. The results (Fig. 11B) indicated a stable generated current density of 10 500 mA m^{-2} in the continuous mode MFC. The current density initially started at around 14 000 mA m^{-2} and experienced a sharp decrease before reaching a stable value after approximately 10 h of operation. The observed initial high current density is likely attributed to the abundance of available substrate (organic matters) and the immediate response of the microorganisms to the nutrient source. As the MFC was initiated, the microorganisms quickly began oxidizing the organic compounds, resulting in a high current density.

However, the subsequent sharp decrease in current density suggests that there may have been limitations in substrate availability or accumulation of byproducts, which hindered the metabolic activity of the microorganisms. The rapid consumption of organic compounds and the establishment of favorable electron transfer pathways may have led to the accumulation of inhibitory byproducts or depletion of essential nutrients, thereby affecting the microbial activity and subsequent power generation.[18,50,55] After the initial decrease, the current density stabilized at 10 500 mA m^{-2}, indicating a balance between substrate consumption and microbial activity. This stable current density suggests that the microorganisms in the MFC reached a steady state, adapting to the operating conditions and establishing a sustainable metabolic activity.

The stability of the generated current density over time demonstrated the viability of the continuous-mode MFC using the graphitized 1100 °C-anode. The stable current density indicates that the microorganisms maintained their electrochemical activity and could efficiently transfer electrons to the anode surface. Furthermore, the continuous addition of sodium acetate at a constant flow rate sustained the microbial activity, allowing for a stable and continuous power output.[56]

The results of this study are valuable for understanding the long-term performance and stability of the MFCs operated in continuous mode. The ability to maintain a stable current density over time is crucial for the practical application of MFCs, given that it ensures consistent power generation and reliable operation. It is worth mentioning that according to our recently published report, which introduced a different

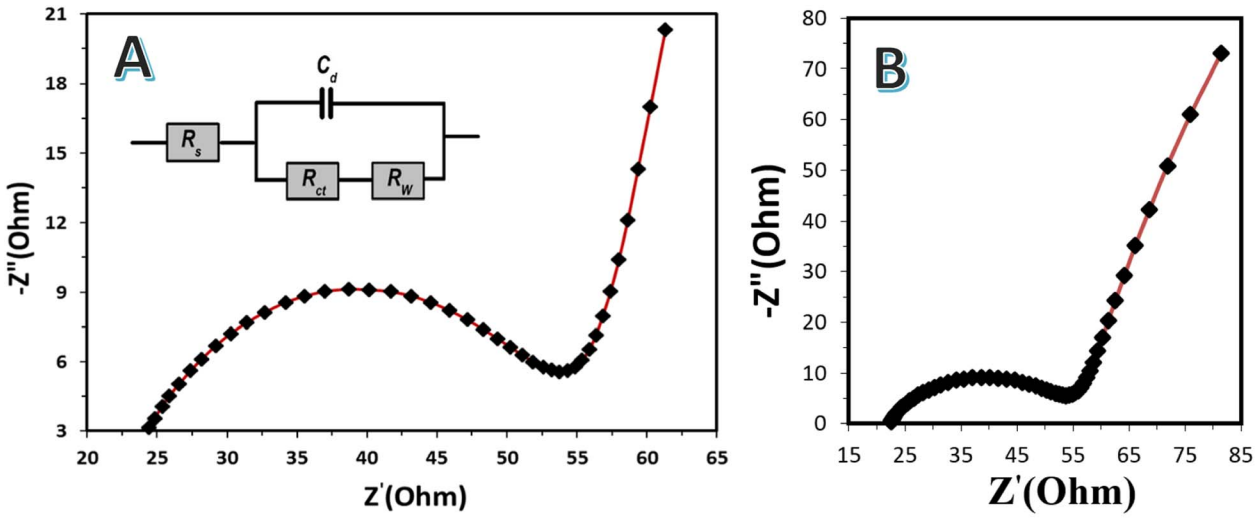

Fig. 10 Electrochemical impedance spectroscopy (EIS) measurements for the 1100 °C (A) and 900 °C (B) mango seed electrodes in a batch mode MFC.

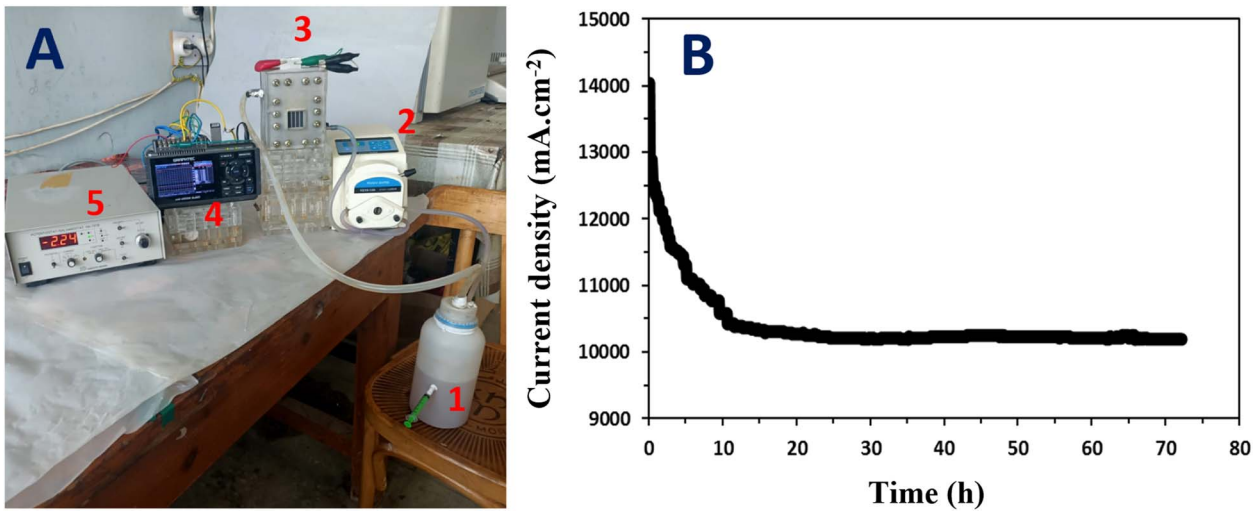

Fig. 11 (A) Photograph of the used continuous-mode MFC using the 1100 °C anode, where the system consists of a storage tank (1), peristaltic pump (2), MFC (3), data logger (4) and potentiostat (5). (B) Generated current density using continuous-mode microbial fuel cell using NaAc (5 g L^{-1})/sewage wastewater analyte at a flow rate of 2 L h^{-1}.

biomass-based anode for MFCs driven by the same wastewater, the generated current density is mainly related to the degradation of organic matter rather than sodium acetate.[38]

3.5 Chemical oxygen demand (COD) removal

The monitoring of chemical oxygen demand (COD) removal over time in the continuous mode microbial fuel cell (MFC) provided important insights into the efficiency of organic substrate degradation and wastewater treatment. To be applicable industrially, the COD removal rate was investigated in the continuous mode MFC assembled with the same above-mentioned process parameters. The removal rate of COD is an important function for the performance of an MFC and a significant parameter for evaluating the utility of this technology for wastewater treatment. Also, it depends on the operating conditions of the reactor, where the final removal of COD is influenced by the hydraulic retention time (HRT) and external load.[57] The analyses were carried out using the HACH Lange LCK514 COD cuvette test and HACH Lange DR3800 spectrophotometer. At the end of the MFC test, the removal percentage of the organic substrate was determined in terms of chemical oxygen demand (COD) using the formula COD removal percentage % = $[(COD_{influent} - COD_{effluent})/COD_{influent}] \times 100$.

As shown in Fig. 12, initially, within the first two days of operation, a slight decrease in COD was observed from 1500 mg L^{-1} to 1475 mg L^{-1}. This minor reduction can be attributed to the slower growth and metabolic activity of the microorganisms during the early stages of the MFC operation.[58,59] As the microbial community established itself and adapted to the environmental conditions, the initial decrease in COD reflects the initial utilization of organic substrate by the microorganisms.

After the initial period, a sharp decrease in COD was observed, reaching a level of 220 mg L^{-1} after six days of operation. This significant reduction indicates a high degree of organic substrate removal, corresponding to approximately 85% COD removal rate. The sharp decrease in COD suggests the efficient degradation of organic compounds present in the wastewater by the microorganisms inhabiting the MFC anode.

The COD removal rate observed in the MFC indicates its potential as a viable technology for wastewater treatment. The microorganisms, driven by the supplied organic pollutants, actively consume and degrade the undesired compounds present in the wastewater, leading to a substantial reduction in COD levels. The efficient removal of COD highlights the capability of MFCs to effectively treat and remediate organic-rich wastewater streams. Furthermore, after the initial sharp decrease in COD, the system reached a steady-state condition. This implies that the microbial community established a balanced metabolic activity, adapting to the continuous

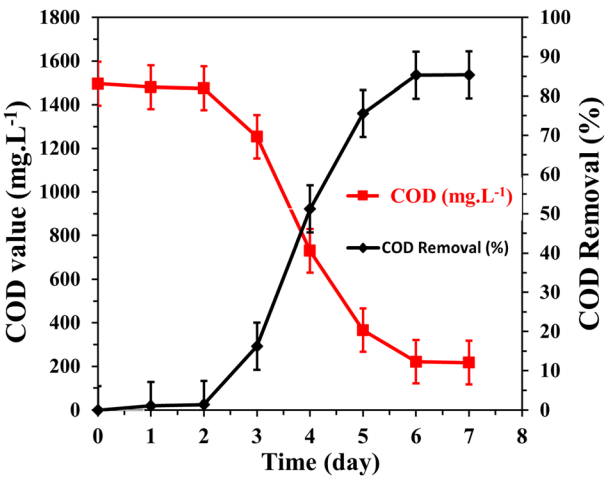

Fig. 12 Change in COD removal with time using continuous mode MFC driven by NaAc (5 g L^{-1})/sewage wastewater anolyte and 1100 °C-mango seed packed anode structure with a flow rate of 2 L h^{-1}.

Table 3 Comparison of the present anode with recently reported biomasses-driven anodes

Biomass source	Organic substrate	Cell configuration	Cathode	Power density	Reference
Coconut shell	Acetate	Single chamber	Air cathode	1069 ± 15 mW m^{-2}	60
Packed sugarcane	Acetate	Double chamber	$K_3Fe(CN)_6$	59.94 ± 2.81 W m^{-3}	31
Loofah sponges	Acetate	Single chamber	Air-cathode	0.82 mW cm^{-3}	61
Bread	Acetate	Double chamber	$K_3Fe(CN)_6$	134 mW m^{-2}	12
Corncob	Acetate	Single chamber	Air cathode	458.85 mW m^{-3}	62
Cocklebur fruit	Acetate	Single chamber	Air cathode	623.24 ± 37.49 (μW)	36
Cocklebur fruit	Acetate	Single chamber	Air cathode	572.57 ± 24 (μW)	36
Activated charcoal	Acetate	Single chamber	Air cathode	562.49 ± 35 (μW)	36
Pinecone	Acetate	Double chamber	$[Fe(CN)_6]$ and KCl	10.88 W m^{-3}	17
Mango wood	Acetate	Single chamber	Air cathode	589.8 mW m^{-2}	5
Oil palm empty fruit bunch waste	Oil palm trunk sap	Single chamber	Air cathode	1350×10^{-3} mW m^{-2}	63
Carbon fiber brush	Acetate	Single chamber	Air cathode	156 mW m^{-2}	64
Grape marc	Acetate	Single chamber	Air cathode	274.9 mW m^{-2}	65
Carbon felt	Acetate	Single chamber	Air cathode	8.8 ± 0.5 W m^{-2}	66
Carbon felt	Acetate	Single chamber	Air cathode	3.1 ± 0.1 W m^{-2}	66
Treated carbon felt	Acetate	Single chamber	Air cathode	272.7 ± 1.5 mW m^{-2}	67
Graphite felt	Acetate	Double chamber	$K_3Fe(CN)_6$	129.81 mW m^{-2}	68
Chinese dates	Acetate	Double chamber	$K_3Fe(CN)_6$	12.17 W m^{-3}	69
Carbonized corncob	Sewage wastewater	Single chamber	Air cathode	2010 mW m^{-2}	38
Packed mango seed	Sewage wastewater	Single chamber	Air cathode	2170.8 mW m^{-2}	This study

supply of organic substrate and effectively degrading it. The stability of COD removal indicates the successful establishment of a functional microbial consortium capable of sustained organic degradation. The results of this study demonstrate the effectiveness of the continuous mode MFC in removing organic pollutants, as indicated by the significant reduction in COD levels. The high COD removal rate observed highlights the potential of MFCs as eco-friendly and sustainable technology for wastewater treatment, offering a promising alternative to conventional treatment methods.

3.6 Comparative analysis with reported biomass-driven anodes

Table 3 provides a comprehensive comparison between the power density obtained from the proposed graphitized mango seed anode and several recently reported biomass-driven anodes used in microbial fuel cells (MFCs). The comparison reveals the exceptional performance of the proposed anode in terms of power density, particularly when considering the specific conditions under which it was tested.

A notable aspect of the comparison is that many of the reported anodes in the table utilized chemical compounds, such as potassium ferricyanide, as electron acceptors. The use of these compounds can significantly increase the cell voltage, and subsequently enhance the power density. In contrast, the proposed anode in this study employed atmospheric oxygen as the electron acceptor, which is a more sustainable and environmentally friendly approach. Also, despite this difference, the generated power density from the proposed anode remains highly competitive, surpassing that of almost all the reported anodes. Furthermore, it is important to note that the majority of the reported anodes were tested using simulated anode chamber solutions, such as acetate, as a source of organic substrate. These solutions are specifically designed to provide optimal conditions for the microorganisms and promote high power output. In contrast, the proposed anode in this study was tested with real sewage wastewater without any pretreatment or addition of external microorganisms. This highlights the robustness and effectiveness of the proposed anode in utilizing complex and diverse organic substrates present in real-world wastewater.

The significantly higher power density obtained from the proposed anode, despite the utilization of complex sewage wastewater and the absence of pretreatment or external microorganisms, is a remarkable achievement. This demonstrates the potential of utilizing agricultural biomass waste, such as mango seeds, as a viable and efficient carbon source for anodes in MFCs driven by sewage wastewater. The high power density achieved underscores the effectiveness of the proposed anode in facilitating efficient electron transfer and power generation from organic substrates in a sustainable and environmentally friendly manner.

The results presented in Table 3 highlight the competitive performance of the proposed anode compared to other biomass-driven anodes reported in the literature. The ability to generate a higher power density while utilizing real wastewater and atmospheric oxygen as an electron acceptor showcases the practicality and potential of the proposed anode for real-world applications. This study contributes to advancing the field of MFC technology by demonstrating the efficacy of utilizing agricultural biomass waste for power generation and wastewater treatment.

4. Conclusion

In conclusion, this study investigated the use of graphitized mango seed as a 3D anode in microbial fuel cells (MFCs) driven

by sewage wastewater. The obtained results provide valuable insights into the performance and potential applications of the proposed anode material. The surface morphology analysis revealed that the graphitized mango seed anode possessed a highly porous structure with layered branches, providing ample surface area for biofilm formation and microorganism attachment. The electrical conductivity measurements demonstrated the efficient electron transfer process, with the investigated samples exhibiting a low electrical resistance. The MFCs assembled with the graphitized mango seed anodes achieved high power densities, with the maximum values observed for the anodes calcined at temperatures of 1100 °C and 1000 °C, respectively. Furthermore, the power density and current density were observed to be stable after an initial stabilization period, indicating the establishment of a stable microbial community and efficient electron transfer network. The continuous mode MFC, utilizing the 1100 °C-anode, demonstrated a stable generated current density over an extended period. Furthermore, the graphitized mango seed anode exhibited impressive chemical oxygen demand (COD) removal capabilities, reaching approximately 85% removal rate within six days of operation. The comparison with reported biomass-driven anodes showcased the superior performance of the proposed anode, even when considering the utilization of real sewage wastewater without pretreatment or external microorganism addition and employing atmospheric oxygen as an electron acceptor. These findings collectively emphasize the effectiveness and potential of the graphitized mango seed anode in MFCs driven by sewage wastewater. The utilization of agricultural biomass waste offers a sustainable and environmentally friendly approach for power generation and wastewater treatment.

Conflicts of interest

The authors declare that they have no conflict of interest.

Acknowledgements

The authors would like to extend their sincere appreciation for funding this research to Researchers supporting project number (RSPD2023R680), King Saud University, Riyadh, Saudi Arabia.

References

1 R. C. Wagner, *Methane Production and Methanogenic Communities in Microbial Electrolysis Cells, Anodic Potential Influence on Microbial Fuel Cells, and a Method to Entrap Microbes on an Electrode*, The Pennsylvania State University, 2012.
2 X. Liu and D. Peng, *Theor. Econ. Lett.*, 2018, **8**, 2220–2232.
3 C. Tortajada, *npj Clean Water*, 2020, **3**, 22.
4 H. Jiang, L. Yang, W. Deng, Y. Tan and Q. Xie, *J. Power Sources*, 2017, **363**, 27–33.
5 M. Li, Y.-W. Li, Q.-Y. Cai, S.-Q. Zhou and C.-H. Mo, *Bioresour. Technol.*, 2020, **300**, 122623.
6 J. M. Dickhout, J. Moreno, P. Biesheuvel, L. Boels, R. Lammertink and W. De Vos, *J. Colloid Interface Sci.*, 2017, **487**, 523–534.
7 S. Li, C. Cheng and A. Thomas, *Adv. Mater.*, 2017, **29**, 1602547.
8 H. Aboutalebi, A. Sathasivan, K. B. Krishna and A. J. Kohpaei, *Bioresour. Technol.*, 2011, **102**, 3981–3984.
9 J. Y. Chen, P. Xie and Z. P. Zhang, *Chem. Eng. J.*, 2019, **361**, 615–624.
10 B. E. Logan, B. Hamelers, R. Rozendal, U. Schröder, J. Keller, S. Freguia, P. Aelterman, W. Verstraete and K. Rabaey, *Environ. Sci. Technol.*, 2006, **40**, 5181–5192.
11 S. Pandit, N. Savla, J. M. Sonawane, A. M. D. Sani, P. K. Gupta, A. S. Mathuriya, A. K. Rai, D. A. Jadhav, S. P. Jung and R. Prasad, *Fermentation*, 2021, **7**, 169.
12 L. Zhang, W. He, J. Yang, J. Sun, H. Li, B. Han, S. Zhao, Y. Shi, Y. Feng and Z. Tang, *Biosensors and Bioelectronics*, 2018, **122**, 217–223.
13 E. Antolini, *Renewable Sustainable Energy Rev.*, 2016, **58**, 34–51.
14 Y. Yuan, S. Zhou, Y. Liu and J. Tang, *Environ. Sci. Technol.*, 2013, **47**, 14525–14532.
15 Y. Wang, C. He, W. Li, W. Zong, Z. Li, L. Yuan, G. Wang and Y. Mu, *Chem. Eng. J.*, 2020, **399**, 125848.
16 M. Lu, Y. Qian, C. Yang, X. Huang, H. Li, X. Xie, L. Huang and W. Huang, *Nano Energy*, 2017, **32**, 382–388.
17 R. Wang, D. Liu, M. Yan, L. Zhang, W. Chang, Z. Sun, S. Liu and C. Guo, *Bioresour. Technol.*, 2019, **292**, 121956.
18 A. A. Yaqoob, M. N. M. Ibrahim and C. Guerrero-Barajas, *Environ. Technol. Innovation*, 2021, **23**, 101579.
19 B. Logan, S. Cheng, V. Watson and G. Estadt, *Environ. Sci. Technol.*, 2007, **41**, 3341–3346.
20 X. Wang, S. Cheng, Y. Feng, M. D. Merrill, T. Saito and B. E. Logan, *Environ. Sci. Technol.*, 2009, **43**, 6870–6874.
21 Q. Deng, X. Li, J. Zuo, A. Ling and B. E. Logan, *J. Power Sources*, 2010, **195**, 1130–1135.
22 S. Cheng and B. E. Logan, *Electrochem. Commun.*, 2007, **9**, 492–496.
23 Y. Liu, F. Harnisch, K. Fricke, U. Schröder, V. Climent and J. M. Feliu, *Biosensors and Bioelectronics*, 2010, **25**, 2167–2171.
24 A. Morozan, L. Stamatin, F. Nastase, A. Dumitru, S. Vulpe, C. Nastase, I. Stamatin and K. Scott, *Phys. Status Solidi A*, 2007, **204**, 1797–1803.
25 M. Di Lorenzo, K. Scott, T. P. Curtis and I. M. Head, *Chem. Eng. J.*, 2010, **156**, 40–48.
26 F. Li, Y. Sharma, Y. Lei, B. Li and Q. Zhou, *Appl. Biochem. Biotechnol.*, 2010, **160**, 168–181.
27 K. Rabaey, P. Clauwaert, P. Aelterman and W. Verstraete, *Environ. Sci. Technol.*, 2005, **39**, 8077–8082.
28 D. Jiang and B. Li, *Biochem. Eng. J.*, 2009, **47**, 31–37.
29 S. Wu, H. Li, X. Zhou, P. Liang, X. Zhang, Y. Jiang and X. Huang, *Water Res.*, 2016, **98**, 396–403.
30 T. Huggins, H. Wang, J. Kearns, P. Jenkins and Z. J. Ren, *Bioresour. Technol.*, 2014, **157**, 114–119.
31 Y. Zhou, G. Zhou, L. Yin, J. Guo, X. Wan and H. Shi, *ChemElectroChem*, 2017, **4**, 168–174.

32 S. You, Q. Zhao, J. Zhang, J. Jiang, C. Wan, M. Du and S. Zhao, *J. Power Sources*, 2007, **173**, 172–177.
33 B. Erable, N. Duteanu, S. S. Kumar, Y. Feng, M. M. Ghangrekar and K. Scott, *Electrochem. Commun.*, 2009, **11**, 1547–1549.
34 M. Di Lorenzo, T. P. Curtis, I. M. Head and K. Scott, *Water Res.*, 2009, **43**, 3145–3154.
35 T. Tommasi, A. Sacco, C. Armato, D. Hidalgo, L. Millone, A. Sanginario, E. Tresso, T. Schilirò and C. F. Pirri, *Chem. Eng. J.*, 2016, **288**, 38–49.
36 C. Yai, M. Chen, Y. Qian, L. Zhang, M. Lu, X. Xie, L. Huang and W. Huang, *Sci. China Mater.*, 2019, **62**, 645–652.
37 B. E. Logan, *Microbial Fuel Cells*, John Wiley & Sons, 2008.
38 N. A. Barakat, M. M. A. Hameed, O. A. Fadali, O. H. Abdelraheem, R. A. Hefny and H. M. Moustafa, *Int. J. Hydrogen Energy*, 2023, **48**, 38854–38869.
39 I. Chakraborty, S. Sathe, B. Dubey and M. Ghangrekar, *Bioresour. Technol.*, 2020, **312**, 123587.
40 T. Wilberforce, M. A. Abdelkareem, K. Elsaid, A. Olabi and E. T. Sayed, *Energy*, 2022, **240**, 122478.
41 C. Torres-León, N. Ramírez-Guzmán, J. Ascacio-Valdés, L. Serna-Cock, M. T. dos Santos Correia, J. C. Contreras-Esquivel and C. N. Aguilar, *LWT*, 2019, **112**, 108236.
42 F. C. S. Vieira and E. Nahas, *Microbiol. Res.*, 2005, **160**, 197–202.
43 J. Li, Y. Gao, K. Han, J. Qi, M. Li and Z. Teng, *Sci. Rep.*, 2019, **9**, 17270.
44 W. K. P. Wickramaarachchi, M. Minakshi, X. Gao, R. Dabare and K. W. Wong, *Chem. Eng. J. Adv.*, 2021, **8**, 100158.
45 J. Liu, Q. Wang, S. Wang, D. Zou and K. Sonomoto, *Biosyst. Eng.*, 2012, **112**, 6–13.
46 W. Zhang, P. Sherrell, A. I. Minett, J. M. Razal and J. Chen, *Energy Environ. Sci.*, 2010, **3**, 1286–1293.
47 L. W. Lai, M. Ibrahim, N. M. Rahim, E. F. Hashim, M. Z. Ya'cob, A. Idris and J. Akhtar, *Cellul. Chem. Technol.*, 2016, **50**, 951–959.
48 K. Subramani, N. Sudhan, M. Karnan and M. Sathish, *ChemistrySelect*, 2017, **2**, 11384–11392.
49 J. Huang, Z. Dong, Y. Li, J. Li, J. Wang, H. Yang, S. Li, S. Guo, J. Jin and R. Li, *Sens. Actuators, B*, 2013, **182**, 618–624.
50 B. E. Logan, *Nat. Rev. Microbiol.*, 2009, **7**, 375–381.
51 C.-C. Fu, C.-H. Su, T.-C. Hung, C.-H. Hsieh, D. Suryani and W.-T. Wu, *Bioresour. Technol.*, 2009, **100**, 4183–4186.
52 Y. Yang, S. Liao, W. Shi, Y. Wu, R. Zhang and S. Leng, *RSC Adv.*, 2017, **7**, 10885–10890.
53 Y. Xiong, J. Qian, Y. Cao, X. Ai and H. Yang, *J. Mater. Chem. A*, 2016, **4**, 11351–11356.
54 K. Li, D. Su, H. Liu and G. Wang, *Electrochim. Acta*, 2015, **177**, 304–309.
55 M. Ramya and P. S. Kumar, *Chemosphere*, 2022, **288**, 132512.
56 F. Zhang, S. Cheng, D. Pant, G. Van Bogaert and B. E. Logan, *Electrochem. Commun.*, 2009, **11**, 2177–2179.
57 X. Zhang, W. He, L. Ren, J. Stager, P. J. Evans and B. E. Logan, *Bioresour. Technol.*, 2015, **176**, 23–31.
58 A. Paitier, A. Godain, D. Lyon, N. Haddour, T. M. Vogel and J.-M. Monier, *Biosens. Bioelectron.*, 2017, **92**, 357–363.
59 S. Sayyah, S. Abd El-Rehim and M. El-Deeb, *Int. J. Polym. Mater.*, 2001, **49**, 59–80.
60 Y. Yuan, T. Liu, P. Fu, J. Tang and S. Zhou, *J. Mater. Chem. A*, 2015, **3**, 8475–8482.
61 L. Zhou, D. Deng, Y. Zhang, W. Zhou, Y. Jiang and Y. Liu, *Biosens. Bioelectron.*, 2017, **90**, 264–268.
62 M. Li, H. Zhang, T. Xiao, S. Wang, B. Zhang, D. Chen, M. Su and J. Tang, *Electrochim. Acta*, 2018, **283**, 780–788.
63 A. A. Yaqoob, M. N. M. Ibrahim, A. S. Yaakop, K. Umar and A. Ahmad, *Chem. Eng. J.*, 2021, **417**, 128052.
64 E. J. R. de Almeida, G. G. Halfeld, V. Reginatto and A. R. de Andrade, *J. Environ. Chem. Eng.*, 2021, **9**, 106221.
65 B. Taşkan, *Environ. Res. Technol.*, 2021, **4**, 108–115.
66 R. Rossi and B. E. Logan, *Chem. Eng. J.*, 2021, **422**, 130150.
67 M. Li, X.-L. Yu, Y.-W. Li, W. Han, P.-F. Yu, K. L. Yeung, C.-H. Mo and S.-Q. Zhou, *Chem. Eng. J.*, 2022, **428**, 130924.
68 S. Qiu, L. Wang, Y. Zhang and Y. Yu, *Int. J. Environ. Res. Public Health*, 2022, **19**, 12297.
69 L. Meng, M. Feng, J. Sun, R. Wang, F. Qu, C. Yang and W. Guo, *Bioresour. Technol.*, 2022, **353**, 127151.